ELSEVIER

Microhardness Testing of Cementitious Materials

S. Igarashi,* A. Bentur,† and S. Mindess‡
*Department of Civil Engineering, Kanazawa University, Japan, †National Building Research Institute-Faculty of Civil Engineering, Technion, Israel, and ‡Department of Civil Engineering, University of British Columbia, Canada

The present paper discusses the underlying principles of microhardness testing, addressing the theoretical background and the testing procedures. The advantage and limitations of this technique are highlighted and on that basis guidelines for its proper use in the research of cementitious systems are presented. For proper microstructural characterization of restricted zones such as the interfacial transition zone (ITZ), there is a special need for adequate preparation of the surface and choice of the right load. For measurements at the ITZ, this load should be in the range of 0.02 to 0.05 N (2 to 5 gmf). The various microhardness profiles obtained next to inclusion surface can be classified and discussed in terms of the influence of a rigid inclusion that should be superimposed on the influence due to a weak ITZ. In the study of the properties of bulk pastes, linear relations were reported between the microhardness value and the compressive strength. The load sensitivity of the microhardness test might be used to generate additional parameters (n, $\ln K_L$) to quantify microstructural characteristics. However, because the interpretation of such parameters is based on empirical relations, they should not be used on their own, but in combination with other test methods. ADVANCED CEMENT BASED MATERIALS 1996, 4, 48–57

KEY WORDS: Cement paste, Interfacial transition zone, Microhardness, Microstructure, Strength

Hardness testing is a common method of evaluating the quality of materials for engineering purposes, in particular metals [1] but also concrete [2]. It is based on forcing an indenter into the surface of the material, by dynamic or static loading, and determining the response in terms of depth of penetration or size of indentation. A variety of test methods have been developed that are considered nondestructive, some of them generic for specific materials such as concrete [3] whereas others are of more general scope. In the past, these tests were applied mainly for quality control and assessment of materials. In recent years, however, there has been an increase in the use of some of these tests for research purposes, due to the development of more sophisticated equipment and better understanding of the physical significance of the hardness value [4–7]. Of particular interest are static tests such as the Vickers test, which although developed for metals is now being increasingly used for research in a range of materials, such as ceramics [4,5] and cement pastes [8–19]. Hardness tests of this kind can be used for evaluating the bulk properties of the material, as well as for determining the mechanical response that is more sensitive to microstructural characteristics. The latter is facilitated when low loads are used and the resulting indentation is not greater than 10–20 μm in length. This is referred to as microhardness.

In view of the greater recognition of the influence of microstructural gradients in cementitious composites on their performance, (that is, the influence of the interfacial transition zone (ITZ) [20,21], there is a need for the development of test methods that can be used to determine the mechanical characteristics of microsize zones in the cementitious systems, in locations that exhibit microstructural gradients. Therefore, microhardness testing that was used in the past mainly as a means for characterizing bulk paste properties in cement pastes [8–10] is now more frequently used to characterize gradients in mechanical properties to better understand their influence [11–19]. Thus, microhardness testing is potentially a powerful tool. Yet, like any other method used for evaluating microstructural effects, it has its limitations, and those limitations should be appreciated if this test method is to be used appropriately.

The object of the present paper is to provide a critical review of microhardness testing and to suggest some guidelines for its proper use in cementitious composites.

Concepts of Hardness Testing

Hardness testing for metallic materials is specified in ASTM E92 [22] and microhardness testing in ASTM

Address correspondence to: Arnon Bentur, National Building Research Institute, Technion Israel Institute of Technology, Technion, Haifa 32000 Israel.
Received August 28, 1995; Accepted March 6, 1996

ISSN 1065-7355/96/$15.00
PII S1065-7355(96)00035-1

E384 [23]. The latter standard does not refer to any specific materials, and the test methods outlined in both standards can also be applied to ceramic and cementitious materials. The test methods in these standards involve static loading, and they address the method of loading, the shape of indenter, and the measurement of hardness. The Vickers test is commonly used for both hardness and microhardness testing in which the indenter has a diamond shape (i.e., square-based pyramid; Figure 1), and the hardness value is defined as the ratio between the load and the contact area of the indentation in units of stress. Other similar tests such as the Knoop, Berkovitch, and Brinnell, use different indenters, and the definition of hardness may sometimes involve the use of the projected surface of the indentation rather than the actual contact surface or the depth of penetration.

The Vickers hardness (H_v) in MPa units is calculated as:

$$H_v = \frac{P}{A_s} = 2P\frac{\sin\left(\frac{\alpha}{2}\right)}{d^2} = 1.8544\frac{P}{d^2} \quad (1)$$

where P = load (N), A_s = surface area of indentation (mm^2), d = mean diagonal of indentation (mm), and α = face of angle of indenter at 136°.

Generally, the hardness is correlated with strength, using the following general relation:

$$H = C\sigma_y \quad (2)$$

where C is constant, known as the constraint factor, and σ_y is yield strength.

The constraint factor for Brinnell, Vickers, and Knoop hardness is often 3 [4]. This value can be shown to be the theoretical value when considering an ideal elastic-plastic material [4]. The region under the indenter consists of an expanding "core" that exerts a uniform hydrostatic pressure on its surrounding; the core is encased in an ideally plastic region within which flow occurs according to some simple yield criterion (Figure 2). Beyond the plastic region lies the elastic matrix. This

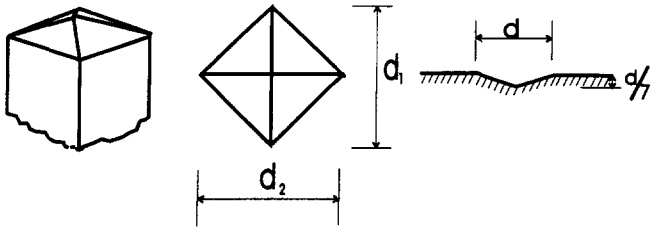

FIGURE 1. Vickers indenter and indentation. d = mean diagonal of indention.

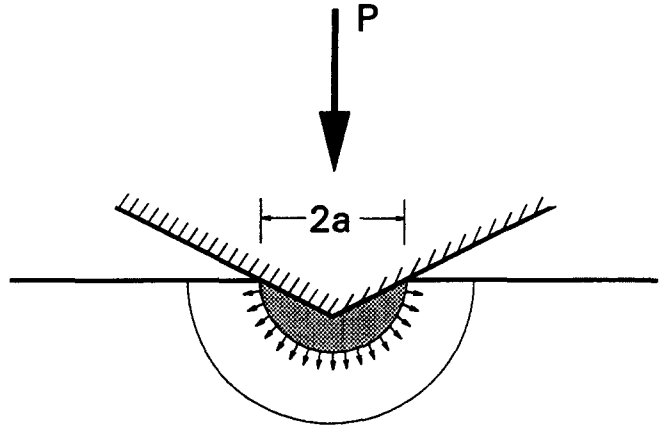

FIGURE 2. Simplified description of the stress field under the indenter assuming elastic-plastic behavior (after Lawn and Wilshaw [7]). P = load; a = half of the indentation diagonal ($d/2$).

description has been shown by Lawn and Wilshaw [7] to be a simplified solution for the more general case of concentrated vertical loading on a semiinfinite space, known as the Boussinesq problem. The solution for this problem in the elastic zone is easily found in textbooks on theory of elasticity. The solution for Cartesian coordinates for the two-dimensional case is shown in Figure 3. Additional details can be found in the reviews by Lawn and Wilshaw [7] that consider the stresses developed beyond the elastic range. For materials like ceramics, which are far from being ideally elastic-plastic, the inelastic deformation was explained by shear-induced flow or pressure-induced densification. Thus, in brittle materials such as cement paste, a mixed mode of fracture by compression and shearing could occur in the region under the indenter. Therefore, the hardness number is not related to strength by a single equation such as eq 2, and the constraint factor can assume values markedly different from 3, both lower and higher. It should be emphasized that since we are dealing with an

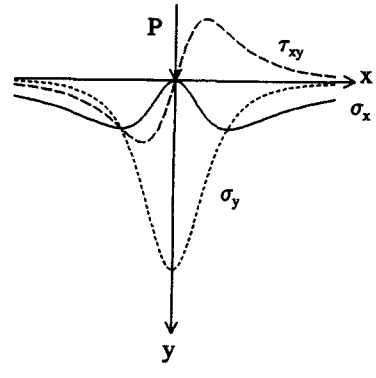

FIGURE 3. Stress distribution is semiinfinite space under concentrated load, assuming ideal elastic behavior. P = load.

indentation induced by stresses that are in the plastic range, the rate of loading and duration of maximum load can affect the size of the indentation. Extensive discussion of these influences is beyond the scope of this paper, and the reader is referred to reference 4 for greater detail.

When considering the stress field, such as shown in Figure 3, one should take into account that the affected volume is considerably greater than the permanent deformation of the impression. Thus, if large inhomogeneities are present, such as hard inclusions (fibers, aggregates), they may provide obstacles to the deformation and affect the entire stress field. This leads to a different hardness value, even if the permanent impression does not overlap the inclusion.

If hardness was a basic material parameter, then tests carried out at different loads would yield the same hardness value (i.e., the ratio P/d^2 in eq 1 would be constant for the same material). However, it is known that in the range of small loads the hardness is dependent on the load, and for many metals it decreases with an increase in load, as shown in Figure 4. The trend may be different with other materials, where hardness might increase with load. It has been shown that when the load is sufficiently high the hardness becomes independent of load. Therefore, it is generally recommended to apply loads in this latter range.

The changes in hardness values in the low-load range occur when the indentation size is of the same order of magnitude as the microstructural features of the tested material, such as grain sizes in metals and ceramics. For example, if the volume affected in the test is smaller than the grain size, the influences of grain boundaries on dislocation movement may be different from those that occur when the affected volume is much greater than the grain size. Therefore, the load variation of hardness, which is called the indentation size effect (ISE), can be a valuable tool for nondestructive testing by providing information that is sensitive to the microstructure of the material. Thus, the field of hardness testing can be divided into three zones (Figure 4): (1) a zone in which hardness is dependent on the load or indentation size, $P < 1$N (0.1 kgf), known as microhardness; (2) a zone in which the hardness is independent of load, $P > 300$ N (30 kgf), known as standard hardness; and (3) a zone in-between, 1 N $< P <$ 300 N, called low-load hardness. The standard hardness range is the one of engineering significance, because it can provide characterization of the bulk properties of the material. The microhardness zone is of significance in research, because it can provide a tool for the detection of microstructural influences. It is perhaps worthwhile to draw attention to an additional zone that is characterized by higher loads, where cracks seem to develop from the edges of the indentation. For engineering purposes, it is recommended that the load lie below this zone. However, there is an increasing amount of work suggesting that the characterization of cracked indents can be useful for the evaluation of fracture mechanics parameters, in particular in brittle solids [6,7]. A few papers have dealt with some of the concepts of the application of this technique to study the fracture mechanics of cement pastes [9,11]. The present paper will deal only with testing in the microhardness range.

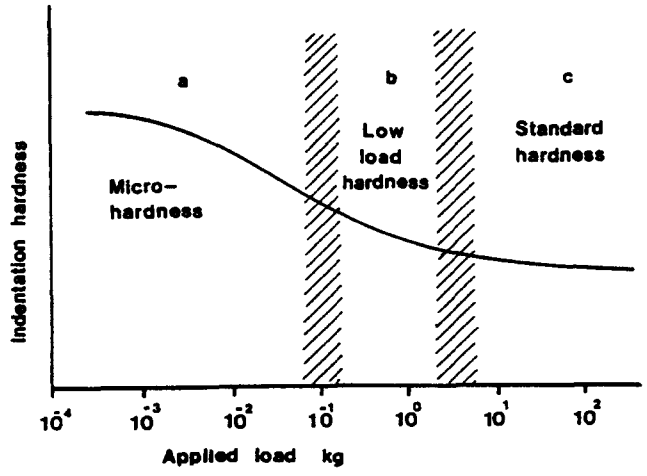

FIGURE 4. Schematic description of the dependence of hardness on the applied load (after McColin [4]).

Microhardness

A common practice of quantifying the ISE in the microhardness range is to determine hardness as a function of load and to plot the data as load versus the mean diagonal of the indentation. Such plots can be described by the following empirical relationship:

$$P = K_L a^n \tag{3}$$

where K_L, n are constants characteristic of the material and a is half of the indentation diagonal ($d/2$).

K_L and n can be found from experimental data by plotting the results in logarithmic form:

$$\ln P = \ln K_L + n \ln a \tag{4}$$

K_L is calculated from the intercept and n from the slope. If n = 2, the hardness is independent of load. The deviation of n from this value is an indication of the ISE. The material constant K_L is the load required to make an indentation of $d = 1$ μm. Because all microhardness indentations are larger than 1 μm, the K_L value is an extrapolated material parameter, useful for comparison but having only a limited significance.

Based on this empirical approach, it was suggested

that microstructural variations of any one material be characterized by assigning to it K_L and n values and presenting the data graphically on n versus $\ln K_L$ plots. A procedure has been developed for calculating the confidence limit of such points [4,5] and presenting it in terms of an ellipsoid surrounding the point on the n versus $\ln K_L$ diagram. An example of such plots for MgO of different grain sizes is given in Figure 5, along with information on other ceramics. It can be seen that n increases towards n = 2 as the MgO grain size decreases. This change towards the limit of n = 2 for "isotropic" polycrystalline behavior reflects the change in the separation between the obstacles providing the impedance to flow, which becomes smaller compared with the scale of indentation as the grain size decreases.

Based on eq 3, a procedure has also been suggested to determine grain sizes in crystalline materials using ln *a* versus ln *P* plots. When the indentation size is smaller than the grain size, a straight line on this plot will result. However, a different straight line will be obtained beyond a certain load limit, when the grain size is smaller than the indentation, and the yield volume sweeps through several boundaries. By resolving the range at which the transformation from one line to the other occurs (Figure 6), the grain size may be estimated [4,5]. Sargent and Page [5] commented that in real materials there are limits to the observable portion of this curve, since indentations made with loads smaller than P_1 may be too small to measure, whereas in a brittle material those made with loads larger than P_2 may result in an indentation that is too cracked to be measured.

It should be noted that such procedures are based on an empirical approach, and there is no unified theory to relate ISE with microstructure. The reason for this is that microstructural influences may result from a variety of effects, and grain size is only one of them. Also, one must consider that the depth of indentation in the microhardness range is small (a few microns or less)

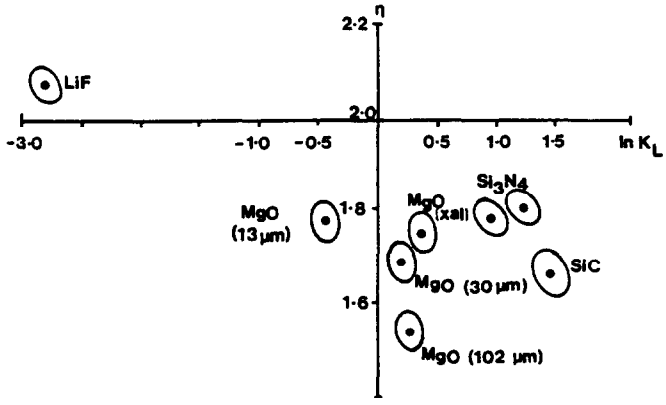

FIGURE 5. n versus $\ln K_L$ plots for MgO of different grain sizes and some other selected ceramics (after Sargent and Page [5]).

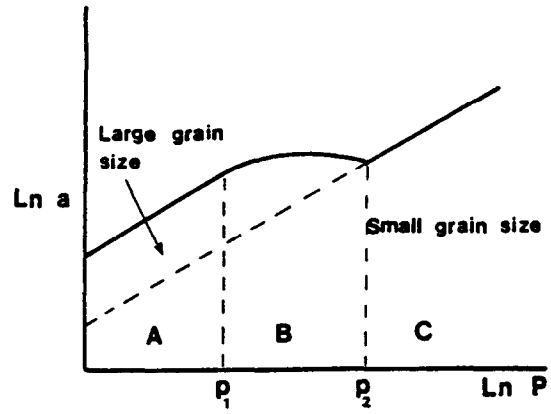

FIGURE 6. Plot of ln*a* versus ln*P* showing the transition zone B where grain size and indent size are comparable (after McColin [4]). *P* = load; *a* = half of the indentation diagonal.

and the indentation may be sensitive to surface influences. For example, polishing of metal to prepare it for microhardness testing may result in a surface layer that is strain hardened. Thus, although this technique is valuable for characterizing microstructural features and mechanical response on the microstructural level, its interpretation should be carried out with some care. It would probably be particularly useful for comparative purposes when studying the same material that has been treated to induce microstructural changes.

Testing Procedures

The Vickers indenter was described in Figure 1. This shape results in an indentation depth that is one-seventh of the diagonals of the indentation. In microhardness testing, the diagonal is usually in the range of 10 to 50 μm. To resolve and measure these diagonals accurately, a flat surface is essential. The preparation of such a surface by cutting, grinding, and polishing is a crucial step in this technique. The degree of surface finish required is dependent of the applied loads, the size of indentation, and the magnification of the observations.

As already discussed, the surface grinding and polishing may affect the measurement, leading to a harder surface in the case of metals, or perhaps a weaker surface in the case of young cement paste, if the surface preparation procedure is too aggressive. Thus, great care should be taken in the preparation of the surface of cement pastes, particularly if they are weak. Practice has shown that, for such materials, cutting with a very good diamond saw is essential. Thereafter, a few minutes of polishing in each step [using polishing powders first of #600 paper (14 μm) and then #1200 paper (5 μm)] may be sufficient to obtain an adequate surface with a minimum of damage.

Procedures for microhardness testing outlined in ASTM E384 [23] are adequate for cement pastes. It should be noted that in view of the sensitivity of the test results to the load applied, one should follow the procedure carefully (in particular maintaining distances between indentation loading points that are at least twice the indentation diagonal) and report the conditions of testing, including the load and the time to full loading, if different from the 10–15 seconds specified in the standards. Unfortunately, this is seldom the case in studies reporting results for cement pastes.

Application of Microhardness Testing to Cement Pastes and Cement Composites

Background

Only few studies have been reported in which microhardness testing was used for evaluating the properties of cementitious materials. They can be divided into two categories:

1. Use of microhardness as a nondestructive test to determine the properties of the bulk paste and to correlate the microhardness values with strength [8–10]. The reason for using the microhardness range in these studies was that it provided a means for testing small and thin specimens that would crack if higher loads were applied.
2. Use of microhardness as a means for characterizing the microstructural gradients in cementitious systems, in particular at the ITZ around inclusions such as aggregates and fibers [12–19].

Testing of Bulk Pastes

The testing of bulk pastes was reported by Beaudoin and Feldman [8] and Feldman and Cheng-Yi [10]. Beaudoin and Feldman [8] found that a linear relationship could be established between microhardness and compressive strength in autoclaved calcium silicate systems (Figure 7), which essentially passed through the origin of the hardness-strength axes. They explained this relationship by showing that both strength and microhardness can be described as logarithmic functions of porosity:

$$\sigma = \sigma_0 \exp(-n' p) \tag{5}$$

where p is porosity and σ_0 and n' are experimental constants.

Some relationships between microhardness and porosity are shown in Figure 8.

Feldman and Cheng-Yi [10] reported on the influence of silica fume in cement pastes on the compressive strength and microhardness values. They also found linear relationships between strength and microhardness (Figure 9) going essentially through the origin, but the correlations were somewhat different for the silica fume pastes and the portland cement paste. For the same compressive strength, the microhardness was slightly higher for the silica fume pastes. Also, it was shown that at early age, the increase in microhardness with curing period was greater in the silica fume pastes than in the cement pastes. Based on microstructural analysis, they also concluded that the silica fume system was more homogeneous.

The microhardness techniques outlined previously were explored in the present work to evaluate the nature of the microstructural changes induced by variations in water to cement (w/c) ratio and addition of silica fume. Microhardness was measured as a function of load. It was shown that the empirical eq 3 was applicable also to cementitious systems (e.g., Figure 10). The values of n and K_L determined by these relationships are plotted in Figure 11 for systems of different

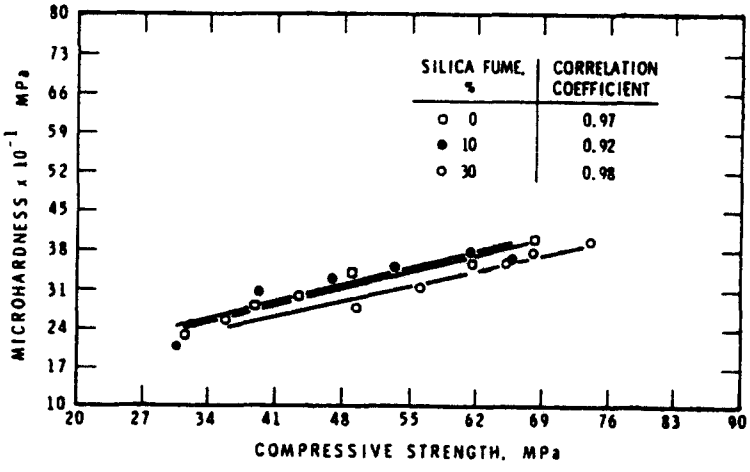

FIGURE 7. Microhardness versus compressive strength for various autoclaved and room temperature cured cement and cement-silica pastes (after Beaudoin and Feldman [8]).

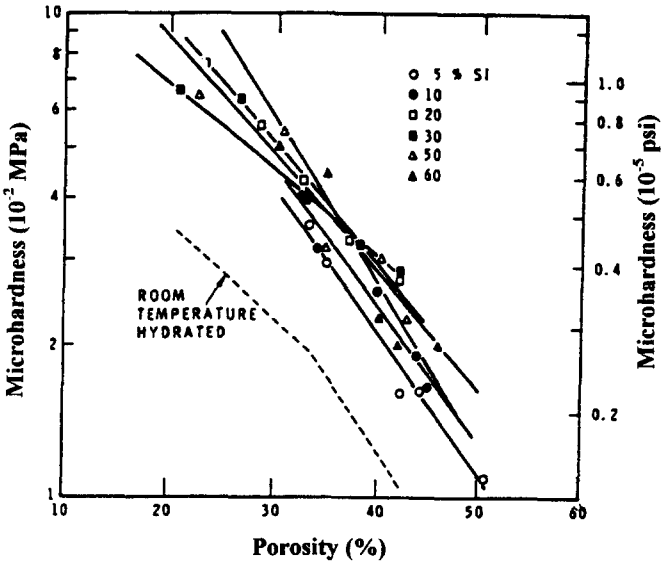

FIGURE 8. Microhardness versus porosity for various autoclaved and room temperature cured cement and cement-silica pastes (after Beaudoin and Feldman [8]).

w/c ratio and silica fume content. It can be seen that, in contrast with metals and many ceramics, n is greater than 2, indicating that an increase in load is associated with increased hardness. One possible explanation is that in these materials the surface is weaker than the bulk; and because for higher loads more of the bulk is affected, the hardness is greater. With regard to this hypothesis, attention should be drawn to the depth of penetration: the indentation diagonals (Figure 10) are in the range of 10 to 30 μm, which implies depths of penetration of about 2 to 5 μm (depth is one-seventh of diagonal). The data showing that microhardness is correlated linearly with compressive strength [8,10] (Figures 7 and 9) suggest that there is no contradiction between the possible sensitivity of microhardness to surface effects and its validity as a measure of bulk properties in the cement paste system. Perhaps both properties are similarly dependent on a common fundamental parameter such as porosity, as supported by the data of Beaudoin and Feldman [8].

It is interesting to note in Figure 11 that for portland cement pastes of low w/c ratio (0.35–0.40), with and without silica fume, the K_L and n values are similar and considerably different than the values of the 0.50 w/c ratio paste. In the latter, the K_L value is smaller and the n value is higher. This difference might be interpreted as reflecting a gross difference in the microstructure of the 0.50 w/c ratio paste, which is expected to contain large capillary pores that are eliminated in well-cured systems having w/c ratios of 0.40 and lower. The decline in the n value towards 2 in the lower w/c ratio pastes may be interpreted as an indication that the microstructure is becoming more homogeneous. This is expected in a system where the large capillary pores are absent.

Microhardness Testing of the ITZ in Cementitious Composites

It is now well established that the cement paste microstructure in the vicinity of the surface of an inclusion is quite different than that of the bulk [20,21]. It is characterized by greater porosity and more heterogeneous microstructure. This zone can extend to distances of about 50 μm from the actual interface and is referred to as the ITZ. Microhardness testing has been reported by several investigators [12–19] as a means of characterizing the properties of this zone relative to the bulk and as a means of estimating its width. The utility of this method is its ability to determine the response to load of a volume element that is considerably smaller than the ITZ. Considering the typical width of the ITZ (50 μm) and the fact that the affected volume is greater than the size of the indentation, the load to be applied in these tests should be such that the indentation size is no larger than 10 to 15 μm in order to be able to map the ITZ with a sufficient number of points (ASTM E384 requires that the spacing between indentation points should be at least two times the diagonal of indentation). On the other hand, applying loads that are too low would result in indentations that are hard to measure accurately. From typical load- and indentation-sized curves (Figure 12) for cement paste, it can be seen that to achieve these conditions the load should not be bigger than 0.05 N (5 gmf) and preferably 0.02 N (2 gmf). Strategies for selecting the indentation points in the measurement of the properties of ITZ are presented in Figure 13. Strategies B and C provide dense mapping, but at the same time assure larger spacings between individual measuring points.

A variety of microhardness profiles have been reported for the ITZ, and some typical examples are given in Figures 14–16. Common to all these results is the observation that in the vicinity of the inclusion surface there is a gradient in the microhardness, but in the bulk paste it becomes relatively constant. The width of the zone in which such gradients exist coincides roughly with the size of the ITZ estimated from direct observations of microstructural gradients. As can be seen in Figures 14–16, the nature of the microhardness gradients can be quite different. Based on the simple description of the ITZ as a zone of higher porosity, the microhardness in this zone should be smaller than that of the bulk. In some test results, such a reduction is observed, but it terminates as the inclusion surface is approached and the microhardness increases to values equal to or greater than those of the bulk paste. Rarely has a trend of consistently lower microhardness, right up to the inclusion surface, been reported. The trends in the gra-

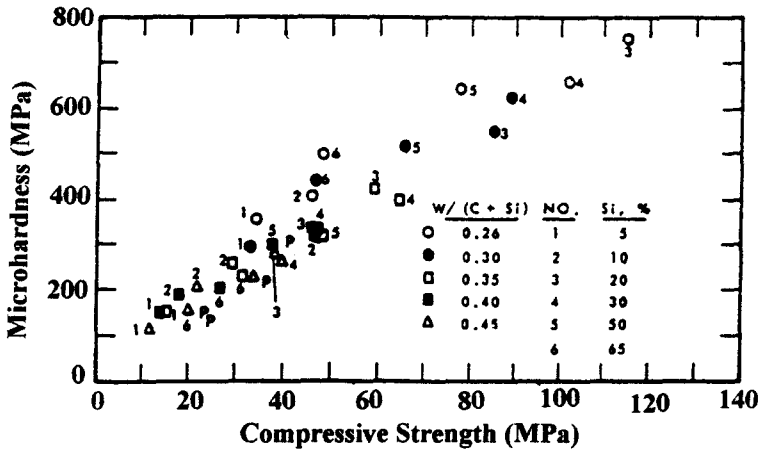

FIGURE 9. Microhardness versus compressive strength for room temperature cured pastes of portland cement with and without silica fume (after Feldman and Cheng-Yi [10]).

dients can be classified into four types as shown in Figure 17. To interpret these gradients properly, it is essential to discuss the possible processes that may lead to their formation. The discussion here is qualitative in nature and will be followed in the future with a quantitative analysis.

Because the volume of the excited material is greater than that of the indentation, the flow of the material under the indentation may be restrained by the presence of a stiff inclusion in its vicinity, as shown schematically in Figure 18a. As a result, the indentation size is expected to be smaller than that of the bulk material away from the inclusion, and the hardness is expected to increase as the inclusion is approached. Two other factors may also lead to an increase in the microhardness of the matrix in the vicinity of the inclusion. Pinchin and Tabor [12] suggested that it may be the result of the presence of large deposits of massive CH; however, they did not show direct evidence to support this hypothesis. If the distance to the inclusion is too small, the downward movement of the indenter may be interrupted as its edge comes into contact with the rigid inclusion (Figure 18b). This, however, is an artifact that can easily be detected by observing whether a fine scratch appears at the edge of the inclusion.

The influences outlined in the previous paragraph may account for the type I curve in Figure 17, which is expected to occur in systems in which (1) the matrix in the vicinity of the inclusion has the same properties as the bulk and the inclusion and the matrix are well bonded at the interface, or (2) the near surface ITZ is rich in massive CH. Deviations from these conditions can lead to changes in the shape of the curve and can account for shapes such as II, III, and IV in Figure 17. If the structure at the ITZ is weaker than that of the bulk matrix and the bond at the actual interface is poor, the shape that will result is IV in Figure 17. If there is a depression in the curve as in II and III, it can be as-

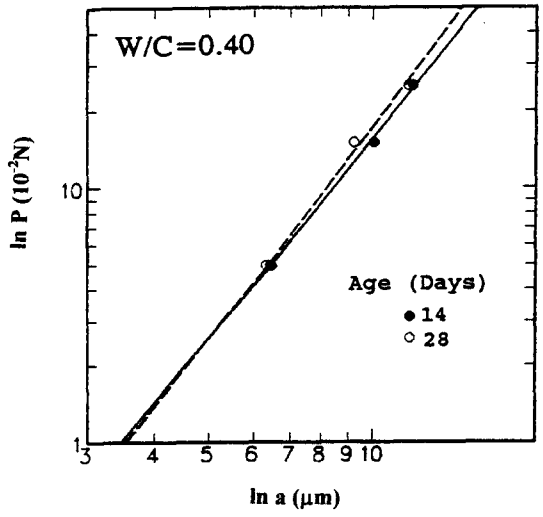

FIGURE 10. ln P versus ln$a$ plots for portland cement pastes cured at room temperature. P = load; a = half of the indentation diagonal.

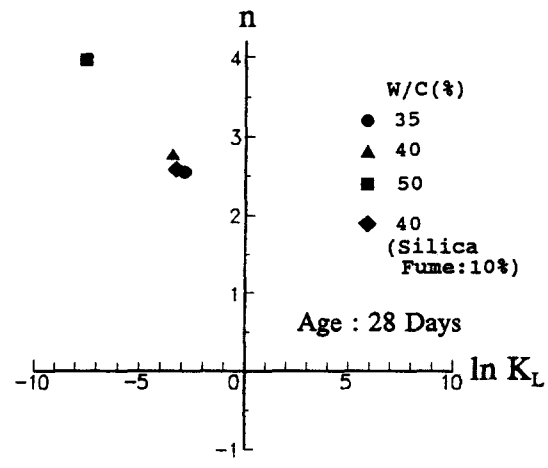

FIGURE 11. n versus ln K_L plots for cement pastes of different water to cement (w/c) ratios, with and without silica fume, cured in water at room temperature for 28 days.

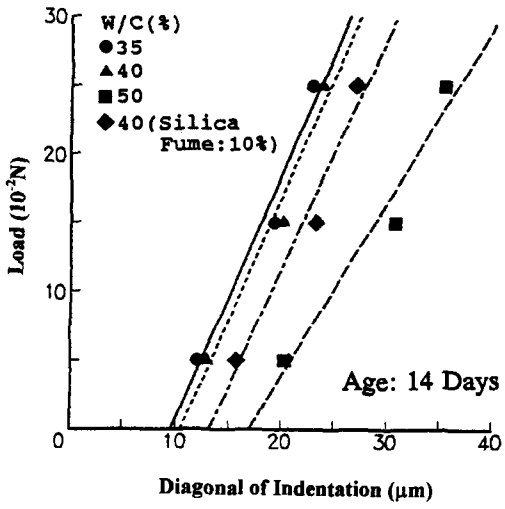

FIGURE 12. Relation between indenter load (P) and indentation diagonal (d) for cement pastes cured at room temperature.

sumed that there is a weak microstructure at the ITZ. The rise in the curve as the inclusion surface is approached can be indicative of at least partial bonding at the interface that enables the inclusion to provide a re-

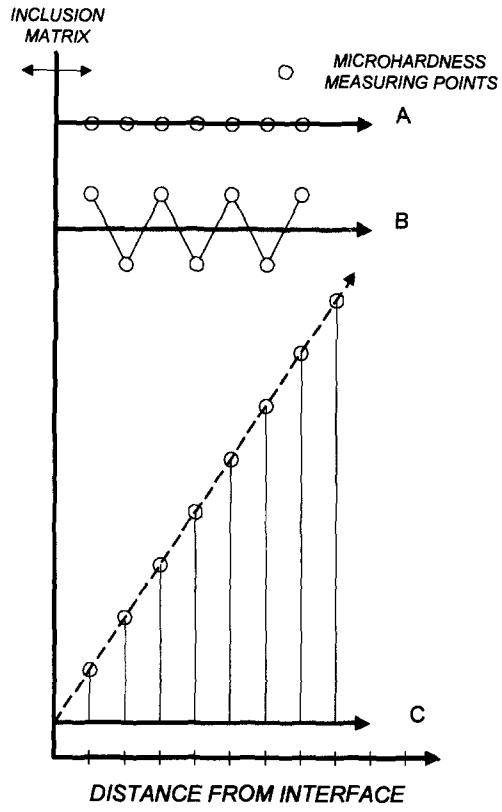

FIGURE 13. Strategies to measure microhardness in the interfacial transition zone (ITZ) in cementitious composites to achieve maximum spacing between indentation points (strategies B and C are preferred).

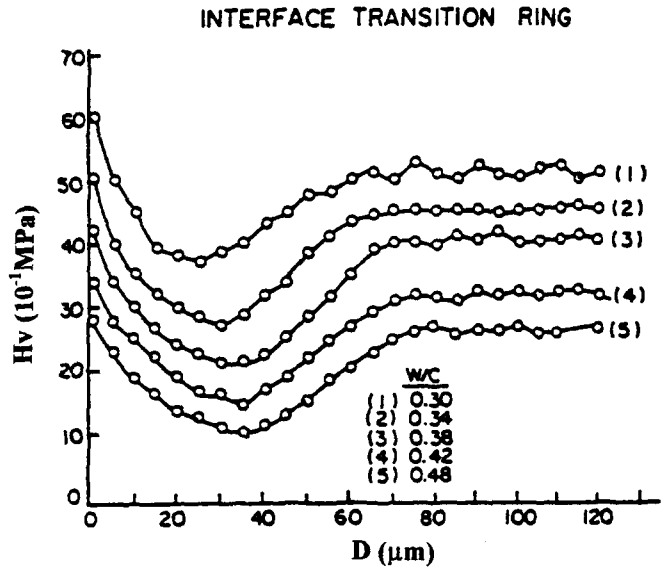

FIGURE 14. Microhardness profiles in the interfacial transition zone (ITZ) of steel fiber pastes of different water to cement (w/c) ratios (after Wei et al. [13]).

straining effect on the indenter or the presence of massive CH. Differences in bonding across the interface can be the result of a variety of factors, such as chemical interaction between the aggregate and the matrix as has been reported for calcite aggregates. In view of such influences, this rise can be at least partly due to an artifact, and, thus, the properties of the matrix at the ITZ cannot be directly quantified in terms of the microhardness value. However, it can provide a qualitative indication of whether the ITZ is weaker than the bulk and give an estimate of the distance over which this weak zone extends into the matrix. Thus, in spite of the

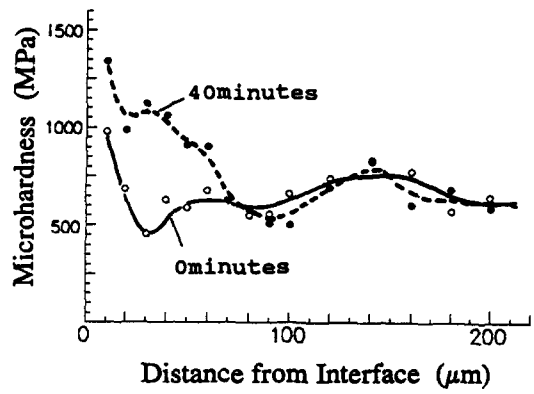

FIGURE 15. Microhardness profiles in the interfacial transition zone (ITZ) of steel fiber-cement paste specimens subjected to different processing in the fresh state: 0 minutes, well-mixed paste cast around a steel fiber; 40 minutes, well mixed-paste cast around a steel fiber. Thereafter, the paste was rotated around the stationary fiber for 40 minutes (adapted from Igarashi et al. [24]).

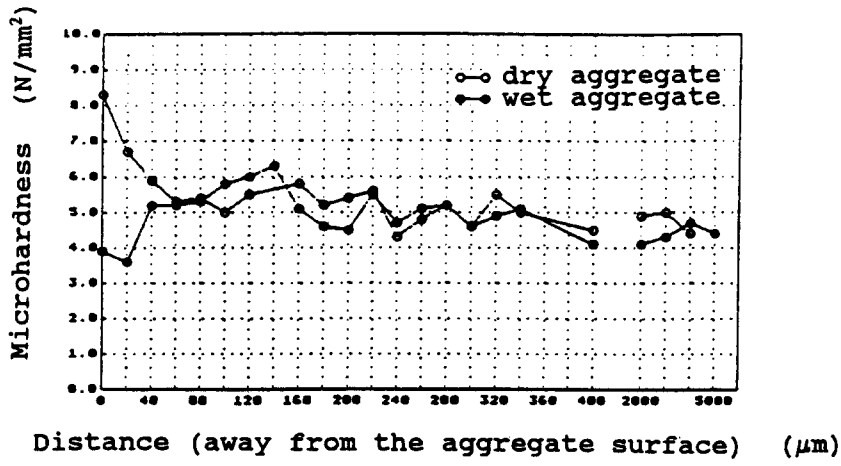

FIGURE 16. Microhardness profiles in the interfacial transition zone (ITZ) of lightweight expanded shale aggregate subjected to different treatments with water prior to casting (after Schneider and Chen [16]).

limitations discussed, the measurement can be useful for qualitative and semiqualitative evaluation. It is particularly beneficial when used for comparative purposes, as in the results shown in Figures 14–16, in which it was applied to study the influence of a change in a single parameter on the ITZ: w/c ratio of the matrix in Figure 14, effect of processing in Figure 15, and effect of water treatment of lightweight aggregate in Figure 16.

The effect of w/c ratio can be interpreted as follows (Figure 14): A decrease in w/c ratio leads to a general improvement in mechanical properties, but the properties of the ITZ are consistently lower than those of the bulk. The fact that the microhardness curve increases towards the inclusion, but does not rise to values higher than those of the matrix, suggests that the interfacial bonding is not as effective as that obtained by special processing, shown in Figure 15.

The effect of processing can be interpreted as follows (Figure 15): Without processing, there is the presence of a weak ITZ, but the rise in the curve towards the aggregate surface suggests that there is some bonding across the interface. In the processed specimen, there seems to be no weak ITZ and the continuous rise in the curve as the aggregate is approached is indicative of efficient bonding across the interface.

The effect of lightweight aggregate treatment with water can be interpreted as follows (Figure 16): In the dry aggregate, the microstructure of the ITZ is as strong or stronger than the bulk matrix, and the bond across the interface is efficient, as seen by the rise in the curve as the aggregate is approached. This may be the result of absorption of water into the aggregate leading to densification of the interfacial matrix and good bonding. In the wet aggregate, the ITZ is poor and the bonding is apparently not sufficiently effective to have an influence of the aggregate, similar to that observed for the dry one.

It should be borne in mind that such interpretations of the microhardness curves are qualitative in nature and based on indirect evidence. To substantiate such analyses, there is a need for complementary data from other techniques, for example, those that will detect the presence or absence of massive CH. Thus, this discussion was intended only to demonstrate the kind of influences that might be resolved with the aid of microhardness techniques if they are applied within the context of a wider range of tests.

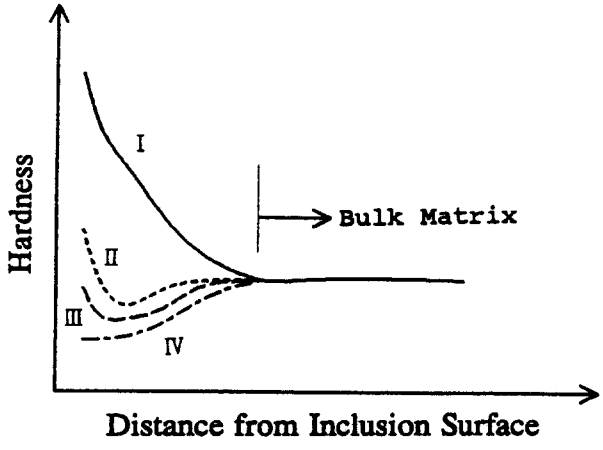

FIGURE 17. Classification of microhardness profile in the interfacial transition zone (ITZ) around a rigid inclusion in a cement paste matrix.

Conclusions

For proper microstructural characterization of restricted zones such as the ITZ, there is a special need for adequate preparation of the surface and choice of the right load. For measurements at the ITZ, this load should be in the range of 0.02–0.05 N (2 to 5 gmf). The various microhardness profiles obtained next to inclusion surface can be classified and discussed in terms of

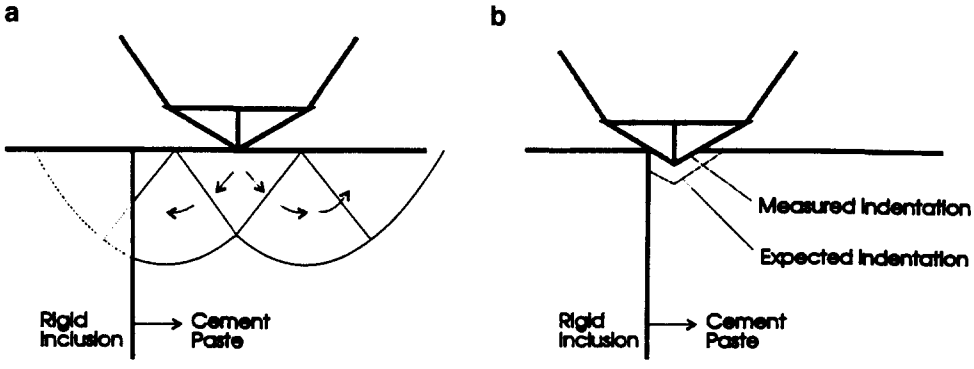

FIGURE 18. Schematic description of the processes that may reduce the penetration of an indenter near a rigid inclusion surface: (a) reduction due to restrain of the stress field, (b) reduction due to physical interaction of the penetrating indenter and the rigid inclusion.

the influence of a rigid inclusion that should be superimposed on the influence due to a weak ITZ.

This method is a valuable one for studying the bulk properties of cement pastes in which linear relationships were reported between microhardness and compressive strength. The load sensitivity of the microhardness test might be used to generate additional parameters (n, $\ln K_L$) to quantify microstructural characteristics. However, because the interpretation of such parameters is based on empirical relations, they should not be used on their own but in combination with other test methods.

Acknowledgments

This work was done at the University of British Columbia. This study was supported by the National Science and Engineering Research Council, through *Concrete Canada*, the Network of Centres of Excellence of High Performance Concrete.

References

1. Boyer, H.E.; Gall, T.L., Eds. *Metals Handbook;* American Society for Metals: Metal Park, 1985.
2. Kholmyanskym, M.; Kogan, E.; Kovler, K. *Materials and Structure* **1994,** *27,* 584–587.
3. Malhotra, V.M.; Carino, N.J., Eds. *Handbook of Nondestructive Testing of Concrete;* CRC Press: Boca Raton, FL, 1991.
4. McColin, I.S. *Ceramic Hardness;* Plenum Press: New York, 1990.
5. Sargent, P.M.; Page, T.F. *J. Br. Ceram. Soc.* **1978,** *26,* 209–224.
6. Lawn, B. *Fracture of Brittle Solids;* Cambridge University Press: Cambridge, England, 1993.
7. Lawn, B.; Wilshaw, R. *J. Mater. Sci.* **1975,** *10,* 1049–1081.
8. Beaudoin, J.J.; Feldman, R.F. *Cem. Concr. Res.* **1975,** *5,* 103–118.
9. Beaudoin, J.J. *Cem. Concr. Res.* **1982,** *12,* 289–299.
10. Feldman, R.F.; Cheng-Yi, H. *Cem. Concr. Res.* **1985,** *15,* 943–952.
11. Mehta, P.K.; Monteiro, R.J.M. In *Materials Research Society Symposium Proceedings 114;* Mindess, S.; Shah, S.P., Eds. Materials Research Society: Pittsburgh, 1988; pp 65–75.
12. Pinchin, D.J.; Tabor, D. *Cem. Concr. Res.* **1978,** *8,* 15–24.
13. Wei, S.; Mandel, J.A.; Said, S. *Am. Concr. Inst. J.* **1986,** *83,* 597–605.
14. Igarashi, S.; Kawamura, M. *Cem. Concr. Res.* **1994,** *24,* 695–703.
15. Kawamura, M.; Igarashi, S. *ASCE J. Mater. Civ. Eng.* **1992,** *4,* 227–239.
16. Schneider, U.; Chen, S. In *Proceedings of the RILEM Symposium;* Maso, J.C., Ed. E&FN Spon: London, 1993; pp 149–156.
17. Qi, Y.; Chu, Q. In *Proceedings of the RILEM Symposium;* Maso, J.C., Ed. E&FN Spon: London; 1993; pp 71–77.
18. Wang, Y. In *Materials Research Society Symposium Proceedings 114;* Mindess, S.; Shah, S.P., Eds. Materials Research Society: Pittsburgh, 1988: pp 49–54.
19. Wang, J.; Liu, B.; Xie, S.; Wu, Z. In *Proceedings of the 8th International Symposium of Chemistry of Cement III;* Brazil, 1986; pp 460–465.
20. Ollivier, J.P.; Maso, J.C.; Bourdette, B. *Adv. Cem. Based Mater.* **1995,** *2,* 30–38.
21. Bentur, A. In *Advances in Cementitious Materials,* Mindess, S., Ed. The American Ceramic Society, 1990; pp 523–550.
22. ASTM E92. Standard Test Method for Vickers Hardness of Metallic Materials.
23. ASTM E384. Standard Test Method for Microhardness of Materials.
24. Igarashi, S.; Bentur, A.; Mindess, S., *Cem. Concr. Comp.,* in press.